Ab Initio Investigation of XCH_2CH_2 and $XCHCH_3$ Radicals (X = F, Cl, Br)

Xuming Zheng and David Lee Phillips*

Department of Chemistry, University of Hong Kong, Pokfulam Road, Hong Kong

Received: September 14, 1999; In Final Form: November 23, 1999

We have done ab initio calculations to find the equilibrium geometries, rotational/inversion barriers, and harmonic vibrational frequencies of several haloethyl radicals (XCH_2CH_2 and $XCHCH_3$ where X = F, Cl, Br). One equilibrium and two transition conformations for XCH_2CH_2 (X = Cl, Br) and $XCHCH_3$ (X = F, Cl, Br) were found on the calculated B3LYP/6-311++G(3df,3pd) potential energy surface. We discuss the effects of the halo substituents on the haloethyl radicals investigated. The C−X bonds of the equilibrium β-haloethyl radicals weaken due to hyperconjugative interaction enhancement as X goes from F to Br. The rotational barriers about the C−C bond have been located using analytical methods. We have also made preliminary vibrational assignments of two bromoethyl radical conformers to experimental transient resonance Raman spectra obtained from the A-band photodissociation of 1-bromo-2-iodoethane.

Introduction

Halo-substituted methyl and ethyl radicals are important reaction intermediates in a range of thermochemical and photochemical processes.[1−11] Experimental investigations of the structures and spectroscopic properties of haloethyl and halomethyl radicals are relatively sparse.[12−25] Electron spin resonance (ESR) spectroscopy[12,13] and microwave spectroscopy[14,15] studies have been used to elucidate the conformational structures of CH_2CH_2F, C_2F_5, CH_2Cl, and CH_2F radicals by analysis of the hyperfine splitting constants and the hyperfine coupling constants. Flash photolysis or pulse radiolysis transient absorption spectroscopy investigations have been done to measure the ultraviolet absorption spectra of CH_2Cl, $CHCl_2$, CH_2Br, and CH_2I.[16−18] Pulse radiolysis or flash photolysis experiments in Ar matrix combined with infrared absorption spectroscopy have been used to acquire the vibrational spectra of CH_2F and C_2F_5.[19−25] While the experimental work is limited, these investigations of haloalkyl radicals directly probe their structures and spectroscopic properties. In addition to the experimental studies, there have been a number of theoretical investigations using ab initio calculations to examine haloalkyl radicals (CH_2F, C_2H_4Cl, C_2H_4F, $C_2H_3F_2$, $C_2H_2F_3$, C_2HF_4, C_2F_5, CH_2Cl, and CH_2Br)[8,26−33] and halocarbenes (CF_2, CCl_2, and CBr_2).[34] In particular, the equilibrium geometries, rotational and inversion barriers, and harmonic vibrational spectra have been calculated for eleven fluorinated ethyl and three chlorinated ethyl radicals using ab initio methods.[28−32] These calculations mainly used UHF/6-31G* level of theory with some MP2 or MP4/6-31G* level of calculations applied to evaluate the geometry or energies of some of the radicals. However, there are few reports of systematic ab initio calculations or experimental structural/spectroscopic studies on the bromine and/or iodine substituted ethyl radicals.[35,36] An ab initio study has been reported for $BrCH_2CH_2$ using a multireference double excitation configuration interaction (MRD-CI) methodology, and this investigation focused on examining the potential energy surface for a possible bridging or shuttling motion of the Br between the two carbon atoms.[37] We have recently observed a transient resonance Raman spectrum of photoproducts produced from the A-band photodissociation of 1-bromo-2-iodoethane in cyclohexane solution.[36] This transient resonance Raman spectrum is probably due to bromoethyl radicals formed from the primary photodissociation of 1-bromo-2-iodoethane.[36]

In this paper we present an ab initio investigation of the structures, vibrational frequencies, and conformational stabilities of several halogenated ethyl radicals: β-haloethyl (XCH_2CH_2) and α-haloethyl ($XCHCH_3$) where X = F, Cl, Br. We have carried out these calculations up to the B3LYP/6-311++G(3df,3pd) level of theory. We compare these results to the corresponding previously investigated fluorinated and/or chlorinated ethyl radicals. We also compare our ab initio results to the experimental transient resonance Raman spectra associated with the A-band photodissociation reaction of 1-bromo-2-iodoethane and make preliminary vibrational assignments to two conformers of bromoethyl radicals.

Calculations

All calculations were done using the *Gaussian 98* program suite.[38] Complete geometry optimizations were performed analytically at UMP2/6-311G(d,p), B3LYP/6-311G(d,p), and B3LYP/6-311++G(3df,3pd) levels of theory. At the optimized geometry for each radical conformer, the harmonic vibrational frequencies were determined by using analytical second derivatives at all stationary points or transition structures. The transition states for 1,2-hydrogen migration between the β-fluoroethyl radical and the α-haloethyl radical were determined using the STQN methods at B3LYP/6-311G(d,p) level of theory.[39]

We have also done ab initio computations to estimate the electronic transition energies as well as the sign and magnitude of the normal mode displacements associated with the excited states of several of the bromoethyl radicals. The relative normal mode displacement Δ_i using the short-time approximation can be given by

$$\Delta_i = k\omega_i^{-3/2}(\partial V/\partial Q_i)_0 \quad (1)$$

* To whom correspondence should be addressed. Fax: 852-2857-1586. E-mail: phillips@hkucc.hku.hk.

10.1021/jp9932721 CCC: $19.00
Published on Web 01/12/2000

TABLE 1: Structural Parameters for the Three Conformations (1a, 1b, and 1c) of the XCH_2CH_2 Radical (X = F, Cl, Br) Found from B3LYP/6-311++G(3df,3pd) Calculations

	X=F			X=Cl			X=Br		
parameters[a]	1a	1b	1c	1a	1b	1c	1a	1b	1c
$R(C_2-C_1)$	**1.476**	**1.474**	**1.475**	**1.455**	**1.476**	**1.460**	**1.426**	**1.474**	**1.434**
$R(X_3-C_2)$	**1.420**	**1.393**	**1.412**	**1.878**	**1.805**	**1.861**	**2.122**	**1.973**	**2.102**
$R(H_4-C_2)$	1.090	1.098	1.089	1.084	1.092	1.084	1.082	1.091	1.081
$R(H_5-C_2)$	1.090	1.098	1.094	1.084	1.092	1.087	1.082	1.091	1.083
$R(H_6-C_1)$	1.080	1.080	1.079	1.080	1.081	1.079	1.080	1.077	1.080
$R(H_7-C_1)$	1.080	1.078	1.080	1.080	1.078	1.080	1.080	1.082	1.080
$A(C_1-C_2-X_3)$	**110.1**	**111.0**	**110.7**	**110.0**	**112.8**	**110.6**	**108.1**	**112.9**	**108.2**
$A(C_1-C_2-H_4)$	112.3	112.0	112.3	113.9	112.2	113.4	116.2	112.8	113.6
$A(X_3-C_2-H_4)$	106.1	107.1	107.1	103.5	106.0	104.2	100.2	105.0	100.2
$A(C_1-C_2-H_5)$	112.3	112.0	111.8	113.9	112.2	113.9	116.2	112.8	116.7
$A(X_3-C_2-H_5)$	106.1	107.1	105.7	103.5	106.0	103.1	100.2	105.0	99.46
$A(H_4-C_2-H_5)$	109.6	107.1	108.8	110.9	107.2	110.7	112.9	107.7	113.6
$A(C_2-C_1-H_6)$	120.6	120.2	121.5	120.4	121.7	121.0	120.6	122.2	121.0
$A(C_2-C_1-H_7)$	120.6	119.8	119.7	120.4	118.7	120.2	120.6	118.4	120.6
$A(H_6-C_1-H_7)$	118.3	120.0	118.8	118.3	119.6	118.8	118.0	119.3	118.4
$D(H_6-C_1-C_2-X_3)$	85.55	0.0	−119.7	84.40	0.0	−116.6	85.11	0.0	−111.4
$D(H_6-C_1-C_2-H_4)$	−156.5	−119.8	0.0	−159.9	−119.6	0.0	−163.2	−118.8	0.0
$D(H_6-C_1-C_2-H_5)$	−32.41	119.8	122.7	−31.31	119.6	127.8	−26.60	118.8	137.5
$D(H_7-C_1-C_2-X_3)$	−85.55	180.0	60.27	−84.40	180.0	63.36	−85.11	180.0	68.63
$D(H_7-C_1-C_2-H_4)$	32.41	60.24	180.0	31.31	60.39	180.0	26.60	61.17	180.0
$D(H_7-C_1-C_2-H_5)$	156.5	−60.24	−57.27	159.9	−60.39	−52.18	163.2	−61.17	−42.48
$\gamma 1$	**8.7**	0.0	0.0	**11.2**	0.0	0.0	**9.8**	0.0	0.0
$\gamma 2$	**54.5**	**56.7**	**55.3**	**51.4**	**55.8**	**50.5**	**42.0**	**54.8**	**41.7**

[a] R = bond length (Å), A = bond angle (deg), D = dihedral angle (deg), γ_1 is the out-of plane angle by the radical site group, γ_2 is the out-of-plane angle by CH_2 group attatched by X atom.

where $(\partial V/\partial Q_i)_0$ is the derivative of the excited electronic state potential energy surface with respect to *i*th normal mode at the ground state geometry. UCIS/6-311G(d,p)//B3LYP/6-311G(d,p), UCIS/6-311++G(3df,3pd)//B3LYP/6-311++G(3df,3pd), RPA/6-311G(d,p)//B3LYP/6-311G(d,p), and RPA/6-311++G(3df,-3pd)//B3LYP/6-311++G(3df,3pd)[40] computations were done to estimate the electronic transition energies. The ground state optimized geometry for the conformation of the bromoethyl radical of interest was found using B3LYP/6-311G(d,p) or 6-311++G(3df,3pd) density functional theory calculations. The normal mode vibrational frequency computations were then done at the ground state optimized geometry for each bromoethyl conformation. The gradient of the potential energy surface of the excited electronic state was obtained using either the CIS or the TD (RPA) calculations, and $(\partial V/\partial Q_i)_0$ can be calculated from projection of the potential energy surface of the excited electronic state at the ground state geometry onto the *i*th ground state vibrational normal mode. In eq 1, the sign of the normal mode displacement is determined by $(\partial V/\partial Q_i)_0$. We used the normal mode displacements found from our ab initio calculations to estimate the relative resonance Raman intensity associated with the electronic transitions of several conformations of the bromoethyl radical using $I_i = \omega_i^2 \Delta_i 2$.

Results and Discussion

***β*-Haloethyl, XCH_2CH_2 (1).** The conformations of the XCH_2CH_2 (X = Br, Cl, and F) radical have been studied using UMP2/6-311G(d,p) and B3LYP/6-311++G (3df,3pd). Figure 1 shows a simple diagram of three conformers (1a, 1b, and 1c) with their atoms numbered 1 through 7, and Table 1 lists their geometric parameters computed from the B3LYP/6-311++G (3df,3pd) level of theory. The difference in the orientation of the *β*-fluoroethyl and *β*-chlorooethyl radicals was discussed in ref 28. On the calculated UHF/6-31G* potential energy surface,[28] the $ClCH_2CH_2$ radical has one equilibrium conformation, 1a, and one transition conformation, 1b, with the equilibrium 1a radical having the orientation of the C−Cl bond eclipsed with the singly occupied molecular orbital (SOMO). However, the FCH_2CH_2 radical has two equilibrium structures and two transition conformations, with the more stable equilibrium structure having the C−H bond eclipsed with the SOMO. The $BrCH_2CH_2$ radical has one equilibrium conformation, 1a, and two transition conformations, 1b and 1c, on the B3LYP/6-311++G(3df,3pd) potential energy surface. Table 1 shows that the C−X and C−C bond lengths, and the CCX bond angle changes between 1a and 1b conformations of $BrCH_2CH_2$ are larger than the corresponding changes in the conformations of the $ClCH_2CH_2$ radical. This suggests that the hyperconjugative interaction tends to increase in strength as the halogen atom changes from F to Br for the *β*-haloethyl radicals.

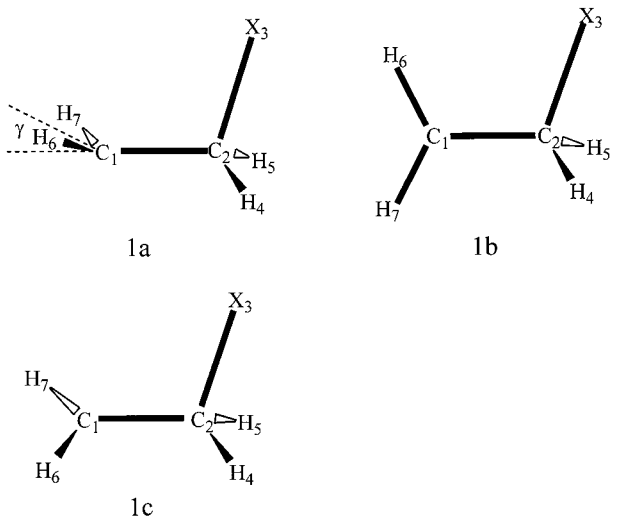

Figure 1. Diagrams of the ground-state XCH_2CH_2 radicals: equilibrium geometry, 1a; transition state geometries, 1b and 1c.

The *β*-haloethyl 1a radical has a nonplanar radical center. The out-of-plane angles γ_1 and γ_2 decrease as X goes from F to Br (Table 1). The decrease in the γ_2 values suggests that the sp^3 hybrid orbital of the *β*-carbon in the *β*-bromoethyl 1a radical

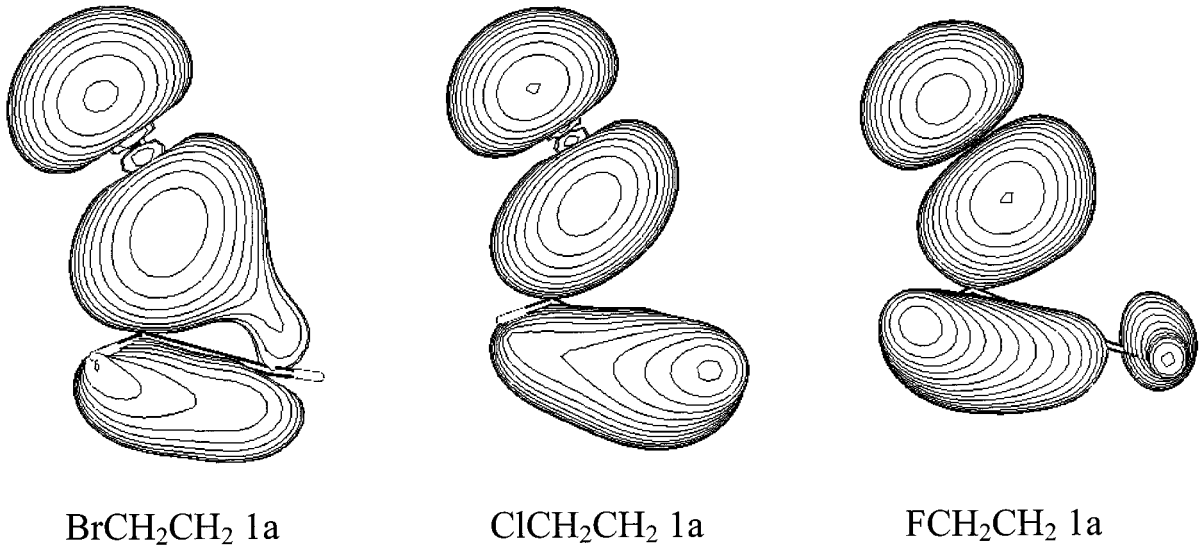

Figure 2. The σ_{C-X} orbital space plots of the equilibrium conformation 1a of the XCH_2CH_2 (X = F, Cl, or Br) radicals using a space contour value of 0.05.

TABLE 2: Calculated Energies (hartrees) of the XCH_2CH_2 (X = F, Cl, Br) Radicals

level of theory	1a	1b	1c	ΔE(1b−1a)	ΔE(1c−1a)
		$BrCH_2CH_2$			
		energy (hartrees)		rotational barrier (kcal/mol)	
UMP2/6-311G(d,p)	−2650.80805	−2650.80302	−2650.80636	3.16 (2.2)	1.06 (0.5)
B3LYP/6-311++G (3df,3pd)	−2652.74480	−2652.73628	−2652.74263	5.34 (4.4)	1.36 (1.1)
		ZPVE[a] (kcal/mol)			
UMP2/6-311G(d,p)	33.2	32.2	32.7		
B3LYP/6-311++G (3df,3pd)	32.4	31.4	32.1		
		$ClCH_2CH_2$			
		energy (hartrees)		rotational barrier (kcal/mol)	
UMP2/6-311G(d,p)	−537.95712	−537.95404	−537.95602	1.93 (1.1)	0.69
B3LYP/6-311++G (3df,3pd)	−538.82058	−538.81625	−538.81928	2.72 (1.9)	0.82 (0.5)
		ZPVE[a] (kcal/mol)			
UMP2/6-311G(d,p)					
B3LYP/6-311++G (3df,3pd)	32.6	31.8	32.3		
		FCH_2CH_2			
		energy (hartrees)		rotational barrier (kcal/mol)	
UMP2/6-311G(d,p)	−177.96811	−177.96804	−177.96796	−0.05 (−0.7)	−0.10
B3LYP/6-311++G (3df,3pd)	−178.46005	−178.46013	−178.46017	−0.05 (−0.6)	−0.07 (−0.2)
		ZPVE[a] (kcal/mol)			
UMP2/6-311G(d,p)					
B3LYP/6-311++G (3df,3pd)	33.2	32.6	33.0		

[a] Zero point vibrational energy. Data in parentheses are the values including the term Δ(ZPVE) × 0.9 for UHF, 0.96 for UMP2, and 1.0 for B3LYP with the torsional frequency excluded.

contains more p-orbital component and less s-orbital component than the corresponding haloethyl radicals with F or Cl replacing Br. The decrease in the γ_1 angle values reflects the p-orbital character of the SOMO of the α-carbon atom increase as X goes from F to Br. When the sp^3 hybrid orbital of β-carbon atom becomes more perturbed and the p-orbital character of the SOMO of the α-carbon atom increases, the attractive overlap of the two orbitals from α-carbon and β-carbon atoms increases and leads to shorter C−C bond lengths. This is especially true for the $BrCH_2CH_2$ 1a radical where the r_{C-C} bond length shortens further and the γ_1 angle becomes smaller.

Figure 2 displays the σ_{C-X} bonding orbital plots using a space contour value of 0.05. Figure 2 clearly indicates that the σ_{C-X} bonding orbital becomes more diffusive as X goes from F to Br. The σ_{C-Br} bonding orbital in $BrCH_2CH_2$ 1a radical is so diffusive that it even flows into the α-carbon region or the radical site. This suggests that the perturbed sp^3 orbital of the β-carbon interacts not only with the Br atom but also with the α-carbon atom. This behavior is very similar to the hypercarbon structure found in a variety of transient molecular systems.[41] Similarly, the SOMO plots using a space contour value of 0.05 also show greater perturbation of the SOMO orbital (α-C) as X changes from F to Br. These space plots appear to indicate that the perturbed SOMO orbital and the perturbed sp^3 orbital make the C−C bonding more efficient to give rise to a shorter C−C bond length and decrease in the values of the γ_1 and γ_2 angles.

Table 2 lists the numerical values of the total energies and rotational barriers corresponding to the conformations 1a, 1b, and 1c for X = Br, Cl, and F. The effect of electron correlation on the relative energies was previously evaluated for various chloroethyl radicals. Previous studies[28] showed that the electron correlation did not affect the rotational barrier significantly when the calculation level of theory increased from MP2 to MP4 and the geometries optimized at UHF/6-31G* were well described. However, a greater discrepancy was noticed between the calculated rotational barrier and the experimental one.[28] The hindered rotational energy estimated from experimental ESR

TABLE 3: Structural Parameters for the Three Conformations (2a, 2b, and 2c) of the $XCHCH_3$ (X = F, Cl, Br) Radicals (refer to Figure 5) Found from the B3LYP/6-311++G(3df,3pd) Calculations

	2a			2b			2c		
parameters[a]	X=F	X=Cl	X=Br	X=F	X=Cl	X=Br	X=F	X=Cl	X=Br
$R(C_2-C_1)$	1.475	1.479	1.479	1.475	1.481	1.481	1.470	1.478	1.478
$R(X_3-C_1)$	1.352	1.717	1.881	1.350	1.714	1.875	1.349	1.715	1.878
$R(H_4-C_1)$	1.082	1.078	1.078	1.078	1.078	1.078	1.077	1.077	1.077
$R(H_5-C_2)$	1.099	1.097	1.098	1.090	1.088	1.088	1.089	1.090	1.090
$R(H_6-C_2)$	1.089	1.090	1.091	1.095	1.096	1.096	1.096	1.095	1.095
$R(H_7-C_2)$	1.092	1.092	1.092	1.095	1.096	1.096	1.096	1.095	1.095
$A(C_2-C_1-X_3)$	115.7	119.6	119.8	117.8	121.3	121.8	117.1	119.9	120.3
$A(C_2-C_1-H_4)$	124.7	124.1	123.8	128.3	124.0	124.0	128.7	125.1	125.3
$A(X_3-C_1-H_4)$	112.6	114.5	113.7	113.9	114.7	114.1	114.2	115.0	114.4
$A(C_1-C_2-H_5)$	112.1	112.1	112.2	109.6	111.3	111.8	109.7	110.0	109.8
$A(H_6-C_2-H_5)$	107.9	107.8	107.6	107.9	108.0	107.9	108.1	108.1	108.1
$A(H_7-C_2-H_5)$	107.2	106.9	107.0	107.9	108.0	107.9	108.1	108.1	108.1
$A(C_1-C_2-H_6)$	109.8	109.9	109.7	112.1	111.3	111.1	112.0	111.9	112.0
$A(C_1-C_2-H_7)$	111.2	111.6	111.7	112.1	111.3	111.1	112.0	111.9	112.0
$A(H_6-C_2-H_7)$	108.5	108.5	108.5	106.9	106.7	106.7	106.9	106.7	106.7
$D(H_5-C_2-C_1-X_3)$	64.21	67.04	69.75	0.0	0.0	0.0	180.0	180.0	180.0
$D(H_5-C_2-C_1-H_4)$	−84.15	−96.58	−90.38	180.0	180.0	180.0	0.0	0.0	0.0
$D(H_6-C_2-C_1-X_3)$	−175.9	−173.1	−170.7	119.9	120.5	120.6	−59.99	−59.84	−59.92
$D(H_6-C_2-C_1-H_4)$	35.75	23.24	29.16	−60.10	−59.46	−59.35	120.0	120.2	120.1
$D(H_7-C_2-C_1-X_3)$	−55.78	−52.80	−50.35	−119.9	−120.5	−120.6	59.99	59.84	59.92
$D(H_7-C_2-C_1-H_4)$	155.9	143.6	149.5	60.10	59.46	59.35	−120.0	−120.2	−120.1
γ_1	30.8	15.6	18.8	0.0	0.0	0.0	0.0	0.0	0.0
γ_2	58.3	57.8	57.7	56.7	58.3	58.7	57.1	57.3	57.1

[a] R = bond length (Å), A = bond angle (deg), D = dihedral angle (deg), γ_1 is the out-of plane angle by the radical site group, γ_2 is the out-of-plane angle by β-CH_2 group.

experiments for $ClCH_2CH_2$ was about 4−5 kcal/mol, while the calculated one was ∼2 kcal/mol at HF or MP2/6-311G(d,p) level of calculations.[28] However, our calculated rotational barrier was ∼3 kcal/mol for B3LYP density functional theory calculations. This is closer to the experimental value (4∼5 kcal/mol) than the HF or MP2 computations, although there is still about 1 kcal/mol difference. The rotational barriers for FCH_2CH_2 are very similar to each other for the three levels of theory (B3LYP, HF, and MP2 with 6-311G(d,p) basis sets) explored. However, the rotational barriers for the B3LYP/6-311++G(3df,3pd) results for XCH_2CH_2 (X = Cl, Br) are significantly larger than those for the HF or MP2/6-311G(d,p) calculations. The rotational barriers (1b−1a) for $BrCH_2CH_2$, $ClCH_2CH_2$, and FCH_2-CH_2 are 2.22, 1.08, and −0.76 kcal/mol, respectively, at the UMP2/6-311G(d,p) level of theory after ZPVE correction, while those at B3LYP/6-311G(d,p) level are 4.76, 2.42, and −0.77 kcal/mol, respectively. These calculations indicate that the rotational barriers for the XCH_2CH_2 series go from almost free rotation in fluorinated ethyl to a significant hindered rotation in brominated ethyl radicals. The large difference in the rotational barriers can be mostly attributed to the increases in C−C bond order and in the steric repulsion between the C−X bond and the C−H bond as X goes from F to Br. For a given basis set, the B3LYP density function theory calculations show a larger decrease in the radical energy, the C−C bond length, and the CCBr bond angle and a greater increase in the C−Br bond length than the MP2 calculation results. This suggests that the coupling of the SOMO with the σ^*_{C-X} orbital and the electron correlation in the β-haloethyl radicals are better described by the B3LYP calculations than the MP2 calculations. Therefore, the rotational barriers from the B3LYP calculations will be larger and in better agreement with the experimental values than the results from the MP2 calculations.

α-Haloethyl, $XCHCH_3$ (2). The $BrCHCH_3$ radical exists in one equilibrium conformation, 2a, and two transition structures, 2b and 2c, at all the levels of theory we examined, and their structures are shown in Figure 3. Table 3 gives the structural parameters for the conformations of the $XCHCH_3$ radicals and Table 4 lists the total energies and rotational barriers.

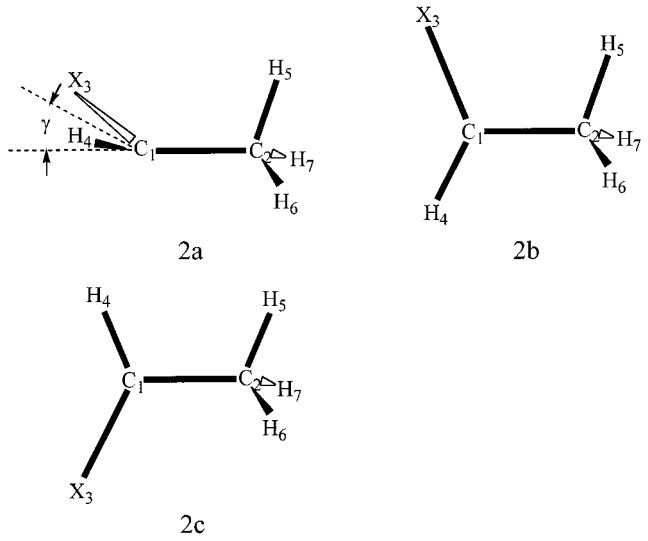

Figure 3. Diagrams of the ground-state $XCHCH_3$ radicals: equilibrium geometry, 2a; transition state geometries 2b and 2c.

The out-of-plane angle γ_1 for $XCHCH_3$ 2a (X = F, Cl, or Br) was 30.8°, 15.6°, and 18.8° for the B3LYP/6-311++G-(3df,3pd) computations (see Table 3), while the corresponding γ_2 was nearly unchanged as X goes from F to Br. γ_2 remains nearly unchanged which suggests that the effect of X on $XCHCH_3$ radicals is mainly localized on the radical site. The change on the γ_1 values for the $XCHCH_3$ radicals comes from the competition between a σ-inductive effect[42] and a π-conjugative interaction.[31] The σ-inductive effect is the interaction of the lowest unoccupied σ-MO with the highest occupied π-MO (SOMO). The π-conjugative interaction is the interaction of a lone pair p orbital of the electronegative atom with the SOMO. The higher electronegativity of the halogen atom favors the σ-inductive effect and makes the α-haloethyl radicals tend

TABLE 4: Calculated Energies (hartrees) of the $XCHCH_3$ (X = F, Cl, Br) Radicals

level of theory	2a	2b	2c	ΔE(2b−2a)	ΔE(2c−2a)
		$BrCHCH_3$			
		energy (hartrees)		rotational barrier (kcal/mol)	
UMP2/6-311G(d,p)	−2650.81081	−2650.80875	−2650.81016	1.29 (0.7)	0.41 (−0.2)
B3LYP/6-311++G (3df,3pd)	−2652.74485	−2652.74361	−2652.74471	0.77 (0.5)	0.08 (−0.3)
		ZPVE[a] (kcal/mol)			
UMP2/6-311G(d,p)	33.2	32.6	32.6		
B3LYP/6-311++G (3df,3pd)	32.1	31.8	31.7		
		$ClCHCH_3$			
		energy (hartrees)		rotational barrier (kcal/mol)	
UMP2/6-311G(d,p)	−537.96275	−537.96059	−537.96217	1.36 (0.7)	0.37 (−0.2)
B3LYP/6-311++G (3df,3pd)	−538.82671	−538.82536	−538.82665	0.85 (0.6)	0.04 (−0.3)
		ZPVE[a] (kcal/mol)			
UMP2/6-311G(d,p)	33.4	32.8	32.8		
B3LYP/6-311++G (3df,3pd)	32.4	32.1	32.0		
		$FCHCH_3$			
		energy (hartrees)		rotational barrier (kcal/mol)	
UMP2/6-311G(d,p)	−177.97590	−177.97170	−177.97348	2.63 (1.5)	1.52 (0.6)
B3LYP/6-311++G (3df,3pd)	−178.46774	−178.46503	−178.46697	1.70 (0.8)	0.48 (−0.2)
		ZPVE[a] (kcal/mol)			
UMP2/6-311G(d,p)	34.4	33.2	33.5		
B3LYP/6-311++G (3df,3pd)	33.4	32.5	32.7		

[a] Zero point vibrational energy. Data in parentheses are the values including the term Δ(ZPVE) × 0.90 for UHF, 0.96 for UMP2, and 1.0 for B3LYP with the torsional frequency excluded.

toward a pyramidal structure, while the lower electronegativity of the halogen atom favors π-conjugative interaction and makes the radical center tend toward a planar structure. Therefore, the degree of nonplanarity increases as the atomic number of halogen substitution increases (from F to Br). Our results generally follow the above theoretical prediction although the magnitude appears noticeably affected by the level of theory. The higher level B3LYP/6-311++G(3df,3pd) calculations give lower γ_1 values than the lower level UMP2/6-311G(d,p) calculations.

The two rotational/inversion transition geometries (2b and 2c) have planar structures with C_s symmetry. For $BrCHCH_3$, the rotational barriers for 2b−2a are 0.691 kcal/mol at UMP2/6-311G(d,p) and 0.48 kcal/mol at B3LYP/6-311++G(3df,3pd), while the rotational barriers for 2c−2a are −0.17 kcal/mol and −0.30 kcal/mol at UMP2/6-311G(d,p) and B3LYP/6-311++G-(3df,3pd), respectively. These results are similar to previous calculations for $FCHCH_3$ and $ClCHCH_3$ explored with UHF or UMP2/6-311G** levels of theory.[28] Examination of the energy difference of the 1a conformation of XCH_2CH_2 and the 2a conformation of $XCHCH_3$ shows that 2a is more stable than 1a by 4.82 kcal/mol for X = F, 3.84 kcal/mol for X = Cl, and 0.03 kcal/mol for X = Br for the B3LYP/6-311++G(3df,3pd) level of computation.

Calculated Vibrational Harmonic Frequencies

There are few reports of experimental infrared or Raman spectra for bromoethyl radicals. We have recently observed a transient resonance Raman spectrum of photoproducts generated from the A-band photodissociation reaction of 1-bromo-2-iodoethane.[36] This transient resonance Raman spectrum may be due to bromoethyl radicals. To help assess this spectrum and provide needed background information for other experimental studies on these haloethyl radicals, we have calculated the harmonic vibrational frequencies. The computed harmonic vibrational frequencies using B3LYP/6-311++G(3df,3pd) computations as well as infrared intensities and Raman intensities using B3LYP/6-311G(d,p) calculations are listed in Tables 5 and 6 for the $BrCH_2CH_2$ and $BrCHCH_3$ radicals.

The dependence of the level of theory on the predicted harmonic vibrational frequencies of radical species (as well as the infrared and Raman intensities) has been extensively investigated.[37,43−47] These studies found that the inclusion of electron correlation effects through second-order Moller−Plesset perturbation theory or density function theory are more efficient in improving the accuracy of the computed spectrum than are HF calculations. We have used UMP2/6-311G(d,p), B3LYP/6-311G(d,p), and B3LYP/6-311++G(3df,3pd) levels of theory to evaluate the vibrational spectra of bromoethyl radicals. Table 5 lists the normal-mode frequencies for β-haloethyl radicals computed using the B3LYP/6-311++G(3df,3pd) level of theory. The B3LYP density function theory calculations give lower C−Br stretch and higher C−C stretch frequencies for the β-bromoethyl 1a radical than do the corresponding UMP2 calculations. Since the B3LYP calculation results in the strongest σ^*_{C-X} hyperconjugative interaction with the radical site SOMO and the lowest total energy among the UHF, UMP2, and B3LYP calculations, we expect that B3LYP density function theory calculation would compute reasonable vibrational frequencies for the β-bromoethyl radicals. The computed vibrational frequencies for the B3LYP/6-311G(d,p) and B3LYP/6-311++G-(3df,3pd) calculations are very similar to one another, and this suggests that the B3LYP/6-311G(d,p) level of theory may also predict reasonable infrared and Raman intensities for the β-haloethyl radicals. Since the bromoethyl 1c radical also has the σ^*_{C-X} hyperconjugative interaction with radical site SOMO, which is similar to the bromoethyl 1a radical, we would expect that the 1c radical has a similar dependence on the level of theory for the computed C−C stretch and C−Br stretch frequencies. The computed frequencies for the bromoethyl 1b radical do not depend very much on the level of theory used since the σ^*_{C-X} hyperconjugative interaction with the radical site SOMO has a lesser role in the transition conformation 1b than in the equilibrium conformation 1a.

All of the bromoethyl radicals have 15 vibrational normal modes. Species with C_s symmetry will separate the 15 modes into 9 modes with A′ symmetry and 6 modes with A″ symmetry. Since the motion associated with each vibrational modes for the bromoethyl radicals found in our calculations at the B3LYP/

TABLE 5: Vibrational Frequencies (cm^{-1}) of the XCH_2CH_2 (X = F, Cl, Br) Radicals (refer to Figure 1) from the B3LYP/6-311++G(3df,3pd) Computation

			1a			1b			1c			
sym		description[a]	X=F	X=Cl	X=Br[b]	X=F	X=Cl	X=Br[b]	sym	X=F	X=Cl	X=Br[b]
A′	ν_1	CH_2 sym str	3148	3152	3153 (118/2.0)	3163	3154	3148 (177/8.7)	A	3153	3155	3155 (129/1.6)
	ν_2	*CH_2 sym str	3052	3104	3132 (91/4.9)	2970	3018	3033 (137/14)		3012	3078	3119 (91/4.8)
	ν_3	*CH_2 def	1512	1504	1513 (9.1/0.1)	1478	1458	1454 (12/2.8)		1500	1490	1501 (9.3/0.6)
	ν_4	CH_2 def	1470	1467	1468 (6.3/8.1)	1440	1445	1444 (7.5/3.6)		1463	1459	1461 (7.3/8.0)
	ν_5	*CH_2 wag	1374	1238	1165 (3.5/4.6)	1397	1310	1264 (7.3/47)		1383	1213	1149 (3.6/2.9)
	ν_6	C−C str	1078	1095	1089 (14/12)	1097	1097	1097 (1.6/0.8)		1066	1099	1108 (15/18)
	ν_7	CH_2 wag	917	689	750 (1.8/68)	1091	984	968 (5.3/7.3)		949	633	692 (1.0/55)
	ν_8	C−X str	650	504	304 (30/17)	868	657	553 (17/17)		596	539	406 (29/20)
	ν_9	CCX bend	389	300	232 (29/31)	432	352	303 (4.0/1.0)		400	316	251 (8.2/11)
A″	ν_{10}	CH_2 asym str	3257	3260	3259 (47/4.4)	3278	3273	3269 (59/1.0)		3263	3265	3263 (55/3.5)
	ν_{11}	*CH_2 asym str	3101	3167	3206 (72/0.2)	2987	3046	3066 (78/5.2)		3088	3157	3201 (67/0.6)
	ν_{12}	*CH_2/CH_2 twist	1274	1255	1244 (1.9/0.1)	1226	1144	1106 (6.8/1.2)		1263	1271	1233 (2.3/2.3)
	ν_{13}	CH_2/*CH_2 twist	1174	1055	994 (2.8/1.4)	950	869	826 (1.3/0.5)		1159	1036	980 (5.5/3.6)
	ν_{14}	CH_2/*CH_2 rock	804	789	787 (0.2/2.8)	430	442	448 (2.8/58)		803	794	782 (1.0/4.0)
	ν_{15}	torsion	86i	234	338 (4.6/0.2)	133i	206i	249i (2.4/3.9)		65i	74	131 (34/17)

[a] *CH_2 denotes the halogen atom X is attached to this group. Here, str = stretch; asym = asymmetric; sym = symmetric; def = deformation. [b] Data in parentheses are the Raman and infrared intensities for the $BrCH_2CH_2$ radicals.

TABLE 6: Vibrational Frequencies (cm^{-1}) of the $XCHCH_3$ (X = F, Cl, Br) Radicals (refer to Figure 4) from the B3LYP/6-311++G(3df,3pd) Computations

			2a			2b			2c		
sym		description[a]	X=F	X=Cl	X=Br[b]	X=F	X=Cl	X=Br[b]	X=F	X=Cl	X=Br[b]
A	ν_1	*CH str	3185	3223	3222 (98/5.2)	3234	3223	3226 (94/5.3)	3241	3234	3239 (96/3.0)
	ν_2	CH_3 str	3105	3095	3089 (105/13)	3104	3113	3113 (58/7.2)	3105	3097	3089 (121/14)
	ν_3	CH_3 str	3046	3040	3045 (117/16)	3012	3016	3014 (129/23)	3003	3020	3022 (90/20)
	ν_4	CH_3 str	2961	2972	2970 (182/23)	2984	2986	2983 (238/26)	2975	2987	2989 (186/20)
	ν_5	CH_3 def	1481	1481	1478 (12/2.8)	1486	1480	1476 (12/6.4)	1484	1483	1480 (11/2.5)
	ν_6	CH_3 def	1458	1462	1459 (13/10)	1458	1465	1465 (13/7.5)	1454	1459	1457 (13/9.5)
	ν_7	CH_3 def	1417	1411	1408 (15/4.6)	1419	1409	1407 (15/3.7)	1423	1412	1408 (15/4.2)
	ν_8	CHX scis	1358	1296	1268 (2.9/59)	1368	1311	1283 (2.0/65)	1358	1292	1261 (3.5/60)
	ν_9	CH_2 wag	1181	1113	1107 (1.8/2.6)	1189	1106	1101 (3.6/1.2)	1191	1115	1108 (1.5/2.1)
	ν_{10}	CH_2 rock	1130	1040	1014 (4.1/14)	1103	1035	1009 (3.0/13)	1135	1045	1020 (3.2/12)
	ν_{11}	C−C str	1014	1000	999 (1.9/0.6)	984	984	976 (1.0/0.7)	996	998	996 (0.6/0.6)
	ν_{12}	C−X str	911	726	623 (6.6/20)	915	723	623 (6.2/16)	913	730	626 (6.7/20)
	ν_{13}	CCX bend	408	360	342 (6.5/32)	447	364	314 (2.9/0.9)	426	349	300 (3.2/0.9)
	ν_{14}	CHX rock	521	287	286 (1.4/7.2)	329i	247	244 (2.1/35)	173	191	176 (0.4/9.2)
	ν_{15}	Torsion	186	137	141 (0.9/0.6)	140i	158i	157i (0.3/4.2)	370i	145i	172i (0.6/34)

[a] *CH_2 denotes the halogen atom X is attached to this group. Here, str = stretch, asym = asymmetric; sym = symmetric; def = deformation. [b] Data in parentheses are the Raman and infrared intensities for the $BrCH_2CH_2$ radicals.

6-311++G(3df,3pd) level of theory is similar to the corresponding chloroethyl radicals, the vibrational assignments of the normal modes are similar to those given in ref 28. Inspection of the MOLDEN animated normal modes for both the equilibrium structures and the transition structures were also used in determining the vibrational assignments.[48]

Electronic States and Photochemistry

Our calculations of the A-band electronic absorption for XCH_2 and two types of bromoethyl radicals are motivated by our recent experimental transient resonance Raman spectrum of photoproducts obtained from the A-band photodissociation of 1-bromo-2-iodoethane.[36] Table 7 presents the calculated electronic absorption bands for halomethyl and bromoethyl radicals. The calculated absorption bands for $ClCH_2$ and $BrCH_2$ radicals agree reasonably well with the previously reported experimental values.[16,17] The calculated absorption bands for the α-bromoethyl radicals are very similar to those for $BrCH_2$ due to their structural similarity. However, the β-bromoethyl equilibrium conformations 1a and 1c have very different calculated absorption bands from the β-bromoethyl 1b radical as well as from the three α-bromoethyl radicals. The first two absorption bands of the β-bromoethyl radical 1a and 1c are located in the 280 ∼ 300 nm region and the third absorption band is in the 255 nm region. The first absorption band of the β-bromoethyl 1b radical and three α-bromoethyl radicals are in the 200 nm to 260 nm region.

Bromoethyl radicals were suggested to contribute to the resonance Raman spectra of 1-bromo-2-iodoethane in cyclohexane solution.[36] We will focus on the transient resonance Raman spectra in the 280 nm to 300 nm region since these spectra are likely to have fewer species contributing to their spectra. The transient 282.4 and 299.1 nm resonance Raman spectra of suspected bromoethyl radicals (obtained from the power dependent resonance Raman experiments mentioned in ref 36) are shown in Figure 4. There are about eight bands (141, 172, 192, 248, 275, 336, 407, and 500 cm^{-1}) observed in the spectra. The β-bromoethyl radicals 1a and 1c are most likely to contribute the transient resonance Raman spectra if only the primary photoproducts and their electronic absorption spectra are taken into consideration. Based on the B3LYP/6-311++G(3df,3pd) calculations, the computed vibrational frequencies of the nominal C−Br stretching, the CCBr bending, and the torsion modes of the β-bromoethyl 1a radical are 304, 232, and 338 cm^{-1}, respectively, and the calculated vibrational frequencies of the nominal C−Br stretch, CCBr bend, and torsion modes

TABLE 7: Calculated and Experimental A-Band Electronic Absorption Bands of the XCH_2 (X = Br, Cl) Radicals and Calculated A-Band Electronic Absorption of the $BrCH_2CH_2$ and $BrCHCH_3$ Radicals

	UCIS/6-311G(d,p) //B3LYP/6-311G(d,p)	RPA/6-311G(d,p) //B3LYP/6-311G(d,p)	exptl (nm)
$ClCH_2$	209 nm *f*=0.0001	214 nm *f*=0.0002	200[a]
	170 nm *f*=0.0000158	172 nm *f*=0.0000	
	158 nm *f*=0.0049	159 nm *f*=0.0016	
$BrCH_2$	244 nm *f*=0.0000	251 nm *f*=0.0000	230[b]
	188 nm *f*=0.0000	193 nm *f*=0.0000	
	180 nm *f*=0.0000	181 nm *f*=0.0000	

	UCIS/6-311G(d,p) //B3LYP/6-311G(d,p)	UCIS/6-311++G(3df,3pd)// B3LYP/6-311++G(3df,3pd)	RPA/6-311G(d,p) //B3LYP/6-311G(d,p)	RPA-6-311++G(3df,3pd) //B3LYP/6-311++G(3df,3pd)
$BrCH_2CH_2$ 1a	293 nm *f*=0.0000	287 nm *f*=0.0002	302 nm *f*=0.0001	298 nm *f*=0.0004
	292 nm *f*=0.0007	286 nm *f*=0.0015	302 nm *f*=0.0010	298 nm *f*=0.0018
	223 nm *f*=0.0160	224 nm *f*=0.0105	253 nm *f*=0.0322	254 nm *f*=0.0244
$BrCH_2CH_2$ 1b	207 nm *f*=0.0000		213 nm *f*=0.0000	
	204 nm *f*=0.0000		210 nm *f*=0.0000	
	181 nm *f*=0.0005		201 nm *f*=0.0000	
$BrCH_2CH_2$ 1c	279 nm *f*=0.0003		288 nm *f*=0.0001	
	277 nm *f*=0.0003		285 nm *f*=0.0001	
	226 nm *f*=0.0082		259 nm *f*=0.0056	
$BrCHCH_3$ 2a	248 nm *f*=0.0024		256 nm *f*=0.0004	
	187 nm *f*=0.0000		192 nm *f*=0.0000	
	173 nm *f*=0.0001		174 nm *f*=0.0000	
$BrCHCH_3$ 2b	263 nm *f*=0.0000		272 nm *f*=0.0001	
	190 nm *f*=0.0000		194 nm *f*=0.0000	
	170 nm *f*=0.0000		171 nm *f*=0.0000	
$BrCHCH_3$ 2c	254 nm *f*=0.0004		262 nm *f*=0.0000	
	187 nm *f*=0.0000		192 nm *f*=0.0000	
	171 nm *f*=0.0000		172 nm *f*=0.0000	

[a] Value from ref 18. [b] Value from ref 19.

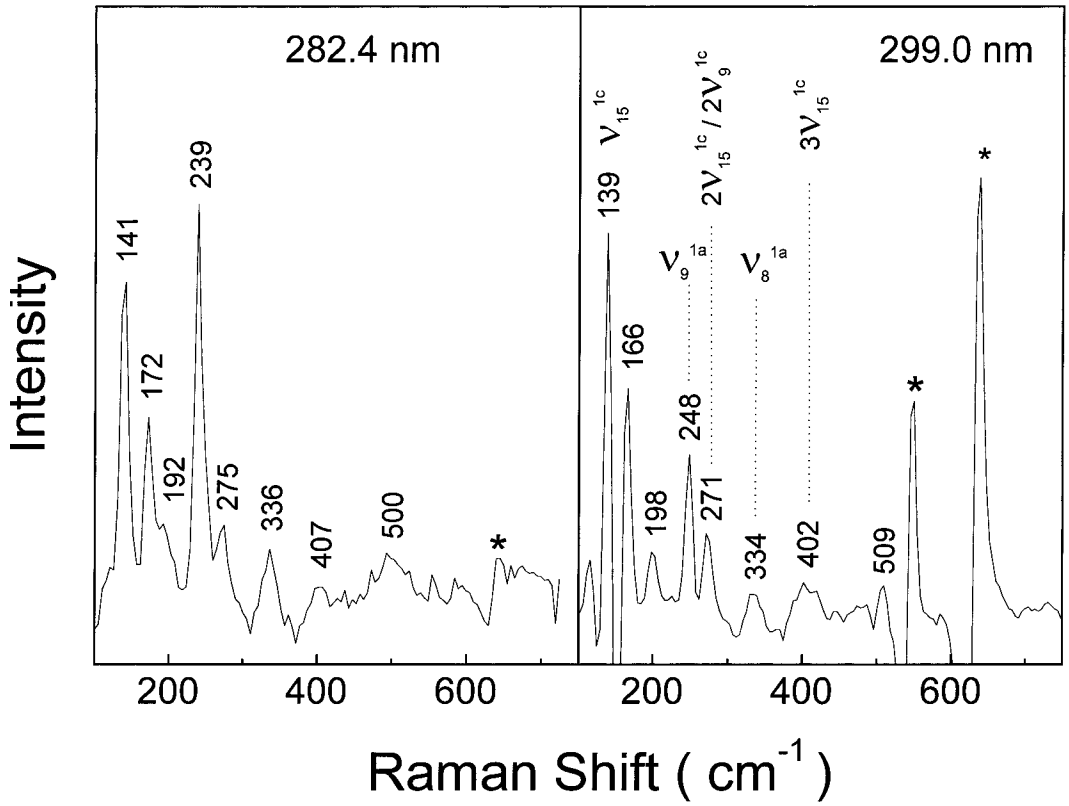

Figure 4. Transient resonance Raman spectra of 1-bromo-2-iodoethane in cyclohexane solution (excitation wavelengths of 282.4 and 299.1 nm).

of the β-bromoethyl 1c radical are 406, 251, and 131 cm^{-1}. We do not consider the transition conformation 1b of β-bromoethyl radical and three conformations of α-bromoethyl radical because their A-band electronic absorptions are far away from the excitation wavelengths used for the resonance Raman experiments. Table 8 lists the relative resonance Raman intensity obtained from our ab initio calculations (see calculation section for details). The reader is also referred to several recent reports for similar types of calculations.[49−51] Table 8 suggests that the 304 and 232 cm^{-1} vibrational modes of the β-bromoethyl 1a radical and the 131, 251, and 406 cm^{-1} vibrational modes of the β-bromoethyl 1c radical are the most probable Franck−

TABLE 8: Ab Initio Calculated Resonance Raman Intensities of the $BrCH_2CH_2$ and $BrCHCH_3$ Radicals (see text for details)

	freq (cm^{-1})	Δ	intensity
$BrCH_2CH_2$ 1a	787	0.00	0.00
	338	0.00	0.00
	304	−0.71	0.87
	232	1.00	1.00
$BrCH_2CH_2$ 1c	782	0.015	0.01
	406	−0.09	0.08
	251	−0.18	0.11
	131	−1.00	1.00
$BrCHCH_3$ 2a	623	−1.00	1.00
	342	0.17	0.01
	286	−0.68	0.10
	141	−0.03	0.00
$BrCHCH_3$ 2b	623	−0.28	0.88
	314	0.60	1.00
	244	0.055	0.005
$BrCHCH_3$ 2c	626	−0.44	0.84
	300	1.00	1.00
	176	0.39	0.05

Condon active modes. Table 8 also shows that the 131 cm^{-1} torsion mode has the largest normal mode displacement and has the largest intensity for the resonance Raman spectra of the β-bromoethyl 1c radical. Therefore, we tentatively assign the observed 141, 275, and 407 cm^{-1} bands to the fundamental, its first overtone, and its second overtone of the torsion vibration mode for the β-bromoethyl 1c radical. The observed 275 cm^{-1} band can also be assigned to the CCBr bending vibration for the β-bromoethyl 1c radical. The observed 248 cm^{-1} band is assigned to the CCBr bending vibration of the β-bromoethyl 1a radical. The experimental 338 cm^{-1} band is tentatively assigned to the C−Br stretching vibration of the β-bromoethyl 1a radical based on the ab initio calculated resonance Raman intensity. However, the large frequency uncertainties that exist between various levels of theory calculations for this vibrational mode make this assignment more uncertain than the others.

1-Bromo-2-iodoethane has two chromophores coupled to each other.[36] It may be possible that both C−I and C−Br chromophores are excited and lead to formation of both bromoethyl radicals and iodoethyl radicals. There may also be secondary reactions occurring during the laser pulse (∼10 ns) to give dihaloethyl products that could also absorb in the A-band absorption. However, the β-bromoethyl radicals appear to be the most likely candidates for the transient resonance Raman spectra. We note that the relative equilibrium population of three β-bromoethyl radicals is 1a:1b:1c = 1:0.0005:0.16, based on a Boltzmann distribution and the calculated energy difference between the 1a, 1b, and 1c conformations. We rule out the β-bromoethyl 1b radical for any noticeable contribution to the observed transient resonance Raman spectra due to its very low population and the fact that its electronic absorption is significantly different from the A-band absorption of 1-bromo-2-iodoethane. Since the relative population of *trans*-1-bromo-2-iodoethane (which correlates to the β-bromoethyl radical 1a) to *gauche*-1-bromo-2-iodoethane (which correlates to the β-bromoethyl 1c radical) is about 70:30, we would expect that the relative population of the β-bromoethyl radical 1a to the β-bromoethyl radical 1c could be between 100:16 to 70:30. During the ns laser pulse, several processes may influence the internal coordinate motions of the β-bromoethyl 1a and 1c radicals detected by the transient resonance Raman spectra. The first process is a bridging or shuttling motion of Br atom between the two carbon center of the β-bromoethyl 1a, postulated by Engel and Peyerimhoff.[38] The calculated energy barrier for Br atom shuttling was calculated to be 1−2 kcal/mol.[38] If this process happens, a large CCBr bending motion (*A′* symmetry) and C−Br motion would be expected to occur. This would give two bands (around the calculated 230 and 300 cm^{-1} frequencies for the CCBr bend and C−Br stretch respectively) and possibly overtones and combination bands as well in the transient resonance Raman spectra. The second process may be a hydrogen atom attached to the β-carbon atom of the β-bromoethyl 1a radical migrating to the α-carbon to form α-bromoethyl 2a radical. The β-bromoethyl 1c radical or other structurally similar radicals may be intermediates during this hydrogen migration between 1a and 2a. Figure 5 shows the Newman projections of the calculated geometry structures for the bromoethyl 1a, 1c, and 2a radicals and corresponding transition state structure for 1,2-hydrogen migration between 1a and 2a (our calculation results at B3LYP/6-311G(d,p) level of theory). Figure 5 illustrates the possible important role of the β-bromoethyl 1c radical or other radicals with structures similar to 1c in the process of the 1,2-hydrogen migration. The computed 1,2-hydrogen migration energy barrier (between ground state 1a or 1c and the transition state) is about 46 kcal/mol (at B3LYP/6-311G(d,p) level of theory). Hamilton and Schaefer[52] carried out the DZ+d CISD calculations for the transition state of the 1,2-hydrogen migration between 1a and 1c of the similar bromoethyl radical cation and predicted that the corresponding energy barrier was 25 kcal/mol. Since an addition of one electron to the three-member ring system of the bromoethyl radical cation destabilizes the radical, a higher hydrogen migration energy barrier for bromoethyl radical than for the corresponding radical cation is expected. The calculated

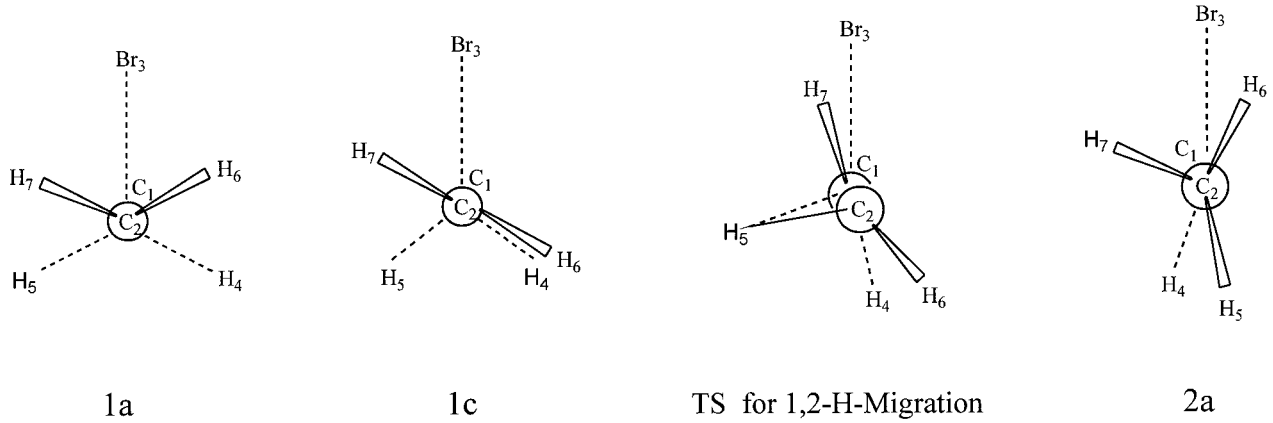

Figure 5. Newmann projections for the geometries of the XCH_2CH_2 radicals 1a and 1c, $XCHCH_3$ radical 2a, and the transition state for the 1,2-hydrogen migration between XCH_2CH_2 1a or 1c and $XCHCH_3$ 2a radicals.

transition energy between the ground state and the first excited electronic state of 1a or 1c is about 99 kcal/mol (~4.2 eV or ~34 000 cm^{-1} photon energy) which is larger than the hydrogen migration energy barrier. Thus, it appears possible for the 1a or 1c radicals to form the 2a radical. If the hydrogen migration between 1a or 1c and 2a happens, we would expect some excitation of the torsional and CCBr bending motion in the β-bromoethyl 1c radical. There are additional processes in which the 1a and 1c radicals could be intermediates.

Our present density functional theory calculations suggest that electron correlation effects are important to take into account for the bromoethyl radicals. The calculations presented here are intended to provide a reasonable estimate of structures, vibrational modes, and electronic transition energies for several haloethyl radicals (in particular bromoethyl radicals) and are not meant to be a complete description of these radicals. It may prove helpful to employ more sophisticated calculations that better account for electronic correlation effects to obtain more accurate estimates of the structures and properties of these haloethyl radicals. We note the caveat that our tentative vibrational assignments of the experimental transient resonance Raman spectra to be primarily due to the bromoethyl radicals 1a and 1c is preliminary in nature. For example, there are two observed frequencies, 172 and 192 cm^{-1}, which are not assigned in this simple consideration that the primary β-bromoethyl 1a and 1c radicals are responsible for the transient resonance Raman spectra. Further work is needed to better establish the exact nature of the photoproduct species from the A-band photodissociation of 1-bromo-2-iodoethane in cyclohexane solution. We are planning to obtain transient resonance Raman spectra with different wavelengths and experimental conditions to help better elucidate the observed photoproduct species. We are also planning to carry out the photodissociation product analysis in order to better correlate the relative importance of the radical 1a and 1c in the process of the photodissociation of 1-bromo-2-iodoethane. It would be very helpful to carry out ultrafast time-resolved spectroscopy studies to monitor in different time scales of the photochemistry of the nascent and later photodissociation products formed in the A-band photodissociation of 1-bromo-2-iodoethane in cyclohexane solution.

Acknowledgment. This work was supported by grants from the Committee on Research and Conference Grants (CRCG), the Research Grants Council (RGC) of Hong Kong, the Hung Hing Ying Physical Sciences Research Fund, and the Large Items of Equipment Allocation 1993-94 from the University of Hong Kong.

References and Notes

(1) Chambers, R. D. Ed.; *Organofluorine Chemistry*; Springer-Verlag: Berlin, 1997.
(2) Kerr, J. A. *Handbook of Biomolecular and Termolecular Gas Reactions Vol. I*; CRC Press: Boca Raton, FL, 1981.
(3) Patai, S.; Rappoport, Z. *Supplement D2 The Chemistry of Halides, Pseudo-Halides, and Azides*; John Wiley & Sons: New York, 1995; Part 2.
(4) Nonhebel, D. C.; Tedder, J. M.; Walton, J. C. *Radicals*; Cambridge University Press: Cambridge, 1997.
(5) Knyazev, V. D.; Bencsura, A.; Dubinsky, I. A.; Gutman, D. *J. Phys. Chem*. **1995**, *99*, 230−238.
(6) Pilgrim, J. S.; Taatjes, C. A. *J. Phys. Chem*. A **1997**, *101*, 4172−4177.
(7) Misochko, E. Y.; Benderskii, A. V.; Wight, C. A. *J. Phys. Chem*. **1996**, *100*, 4496−4502.
(8) Cramer, C. J. *J. Org. Chem*. **1991**, *56*, 5229−5232.
(9) Engels, B.; Peyerimhoff, S. D.; Skell, P. S. *J. Phys. Chem*. **1990**, *94*, 1267−1275.
(10) Bernardi, F.; Bottoni, A.; Canepa, C.; Olivucci, M.; Robb, M. A.; Tonachini, G. *J. Org. Chem*. **1997**, *62*, 2018−2025.
(11) Kambanis, K. G.; Lazarou, Y. G.; Papagiannakopoulos, P. *Chem. Phys. Lett*. **1997**, *268*, 498−504.
(12) Chen, K. S.; Krusic, P. J.; Meakin, P.; Kochi, J. K. *J. Phys. Chem*. **1974**, *78*, 2014−2030.
(13) Meakin, P.; Krusic, P. J. *J. Am. Chem. Soc*. **1973**, *95*, 8185−8188.
(14) Endo, Y.; Yamada, C.; Saito, S.; Hirota, E. *J. Chem. Phys*. **1983**, *79*, 1605−1611.
(15) Endo, Y.; Saito, S.; Hirota, E. *Can. J. Phys*. **1984**, *62*, 1347−1360.
(16) Roussel, P. B.; Lightfoot, P. D.; Caralp, F.; Catoire, V.; Lesclaux, R.; Forst, W. *J. Chem. Soc., Faraday Trans*. **1991**, *87*, 2367−2377.
(17) Villenave, E.; Lesclaux, R. *Chem. Phys. Lett*. **1995**, *236*, 376−384.
(18) Sehested, J.; Ellermann, T.; Nielsen, O. J. *Int. J. Chem. Kinet*. **1994**, *26*, 259−272.
(19) Yamada, C.; Hirota, E. *J. Mol. Spectrosc*. **1986**, *116*, 101−107.
(20) Jacox, M. E.; Miligan, D. E. *J. Chem. Phys*. **1969**, *50*, 3252−3262.
(21) Jacox, M. E. *Chem. Phys*. **1981**, *59*, 199−212.
(22) Raymond, J. I.; Andrews, L. *J. Phys. Chem*. **1971**, *75*, 3235−3242.
(23) Butler, R.; Snelson, A. *J. Fluorine Chem*. **1980**, *15*, 89−102.
(24) Compton, D. A. C.; Rayner, D. M. *J. Phys. Chem*. **1982**, *86*, 1628−1636.
(25) Jacox, M. E. *J. Phys. Chem*. **1984**, *88*, 445−448.
(26) Sekušak, S.; Güsten, H.; Sablijic, A. *J. Chem. Phys*. **1995**, *102*, 7504−7518.
(27) Hopkinson, A. C.; Lien, M. H.; Csizmadia, I. G. *Chem. Phys. Lett*. **1980**, *71*, 557−562.
(28) Chen, Y.; Tschuikow-Roux, E. *J. Phys. Chem*. **1992**, *96*, 7266−7272.
(29) Chen, Y.; Rauk, A.; Tschuikow-Roux, E. *J. Chem. Phys*. **1991**, *95*, 2774−2786.
(30) Chen, Y.; Rauk, A.; Tschuikow-Roux, E. *J. Chem. Phys*. **1990**, *93*, 1187−1195.
(31) Chen, Y.; Rauk, A.; Tschuikow-Roux, E. *J. Chem. Phys*. **1990**, *93*, 6620−6629.
(32) Chen, Y.; Rauk, A.; Tschuikow-Roux, E. *J. Chem. Phys*. **1991**, *94*, 7299−7310.
(33) Cai, Z.-L. *J. Phys. Chem*. **1993**, *97*, 8399−8402.
(34) Russo, N.; Sicilia, E.; Toscano, M. *J. Chem. Phys*. **1992**, *97*, 5031−5036.
(35) Pacansky, J.; Koch, W.; Miller, M. D. *J. Am. Chem. Soc*. **1991**, *113*, 317−328.
(36) Zheng, X.; Phillips, D. L. *J. Chem. Phys*. **1999**, *110*, 1638−1649.
(37) Engel, B.; Peyerimhoff, S. D. *THEOCHEM* **1986**, *31*, 59−68.
(38) *Gaussian 98* (Revision A.7); Frisch, M. J.; Trucks, G. W.; Schlegel, H. B.; Scuseria, G. E.; Robb, M. A.; Cheeseman, J. R.; Zakrzewski, V. G.; Montgomery, J. A., Jr.; Stratmann, R. E.; Burant, J. C.; Dapprich, S.; Millam, J. M.; Daniels, A. D.; Kudin, K. N.; Strain, M. C.; Farkas, O.; Tomasi, J.; Barone, V.; Cossi, M.; Cammi, R.; Mennucci, B.; Pomelli, C.; Adamo, C.; Clifford, S.; Ochterski, J.; Petersson, G. A.; Ayala, P. Y.; Cui, Q.; Morokuma, K.; Malick, D. K.; Rabuck, A. D.; Raghavachari, K.; Foresman, J. B.; Cioslowski, J.; Ortiz, J. V.; Baboul, A. G.; Stefanov, B. B.; Liu, G.; Liashenko, A.; Piskorz, P.; Komaromi, I.; Gomperts, R.; Martin, R. L.; Fox, D. J.; Keith, T.; Al-Laham, M. A.; Peng, C. Y.; Nanayakkara, A.; Gonzalez, C.; Challacombe, M.; Gill, P. M. W.; Johnson, B.; Chen, W.; Wong, M. W.; Andres, J. L.; Gonzalez, C.; Head-Gordon, M.; Replogle, E. S.; Pople, J. A. Gaussian, Inc.: Pittsburgh, PA, 1998.
(39) Peng, C. and Schlegel, H. B. *Isr. J. Chem*. **1994**, *33*, 449.
(40) Bauernscmitt, R.; Ahlrichs, R. *Chem. Phys. Lett*. **1996**, *256*, 454.
(41) Olah, G. A.; Prakash, G. K. S.; Williams, R. E.; Field, L. D.; Wade, K. *Hypercarbon Chemistry*; John Wiley & Sons: New York, 1987.
(42) Pauling, L. *J. Chem. Phys*. **1969**, *51*, 2767−2769.
(43) Yamaguchi, Y.; Frisch, M.; Gaw, J.; Schaefer, H. F.; Binkley, J. S. *J. Chem. Phys*. **1986**, *84*, 2262−2278.
(44) Simandiras, E. D.; Rice, J. E.; Lee, T. J.; Amos, R. D.; Handy, N. C. *J. Chem. Phys*. **1988**, *88*, 3187−3195.
(45) Pacansky, J.; Wahlgren, U.; Bagus, P. S. *Theor. Chim. Acta* **1976**, *41*, 301−309.
(46) Bagus, U. I.; Pacansky, J.; Bagus, P. S. *J. Chem. Phys*. **1975**, *63*, 2874−2881.
(47) Bagus, P. S.; Pacansky, J.; Wahlgren, U. *J. Chem. Phys*. **1977**, *67*, 618−623.
(48) Schafteneaar, G. *MOLDEN*, CAOS/CAMM Center, The Netherlands, 1991.
(49) Stock, G.; Woywod, C.; Domcke, W.; Swinney, W.; Hudson, B. S. *J. Chem. Phys*. **1995**, *103*, 6851−6860.
(50) Markham, L. M.; Hudson, B. S. *J. Phys. Chem*. **1996**, *100*, 2731−2737.
(51) Foley, M. S. C.; Braden, D. A.; Hudson, B. S.; Zgeirski, M. Z. *J. Phys. Chem*. **1997**, *101*, 1455−1459.
(52) Hamilton, T. P.; Schaefer, H. F. *J. Am. Chem. Soc*. **1990**, *112*, 8260−8265.